A MORPHING WING USED SHAPE MEMORY ALLOY ACTUATORS NEW CONTROL TECHNIQUE WITH BI-POSITIONAL AND PI LAWS OPTIMUM COMBINATION

Part 1: Design Phase

Teodor Lucian Grigorie, Andrei Vladimir Popov, Ruxandra Mihaela Botez
École de Technologie Supérieure, Montréal, Québec H3C 1K3, Canada

Mahmoud Mamou, Youssef Mébarki
National Research Council, Ottawa, Ontario K1A 0R6, Canada

Keywords: Morphing Wing, Shape Memory Alloy Actuators, Bi-positional and PI Control Design, Numerical Simulations.

Abstract: The paper presents the design phase of the actuators control system development for a morphing wing application. Some smart materials, like Shape Memory Alloy (SMA), are used as actuators to modify the upper surface of the wing made of a flexible skin. The actuations lines control is designed and validated using a numerical simulation model developed in Matlab/Simulink. The finally adopted control law is a combination of a bi-positional law and a PI law; the control must behave like a switch between cooling phase and heating phase, situations where the output current is 0 A, or is controlled by a law of PI type. The PI controller, for the heating phase, is optimally tuned using the Ziegler-Nichols criterion and the linear model obtained using the System Identification Toolbox of Matlab. The controlled linearized system for heating phase is numerically tested in terms of time response, stability, controllability and the observability. In the actuation control design final phase, numerical simulations, based on SMA non-linear analytical model, were used for validation.

1 INTRODUCTION

Many researches are made around the world in the new challenge field related to the morphing aircraft, with the purpose to improve operational efficiency, particularly by reducing fuel consumption (Chang, 2009, Smith, 2007, Hinshaw, 2009, Gonzalez, 2005, Namgoong, 2006, Majji, 2007, and Ruotsalainen, 2009). Therefore, a lot of architecture were and are still imagined, designed, studied and developed, for this new concept application. One of these is our team project including the numerical simulations and experimental multidisciplinary studies using the wind tunnel for a morphing wing equipped with a flexible skin, smart material actuators and pressure sensors. The aim of these studies is to develop an automatic system that, based on the information related to the pressure distribution along the wing chord, moves the transition point from the laminar to the turbulent regime closer to the trailing edge in order to obtain a larger laminar flow region, and, as a consequence, a drag reduction.

The objective of here presented research work was to develop an actuation control concept for a new morphing mechanism using smart materials, like Shape Memory Alloy (SMA), as actuators. These actuators modify the flexible upper surface of the wing, changing the airfoil shape. The morphing wing project was developed by Ecole de Technologie Supérieure in Montréal, Canada, in collaboration with Ecole Polytechnique in Montreal and the Institute for Aerospace Research at the National Research Council Canada (IAR-NRC).

To achieve the aerodynamic imposed purpose, a first phase of the studies involved the determination of some optimized airfoils available for 35 different flow conditions (five Mach numbers and seven angles of attack combinations). The optimized

Lucian Grigorie T., Popov A., Mihaela Botez R., Mamou M. and Mébarki Y. (2010).
A MORPHING WING USED SHAPE MEMORY ALLOY ACTUATORS NEW CONTROL TECHNIQUE WITH BI-POSITIONAL AND PI LAWS OPTIMUM COMBINATION - Part 1: Design Phase.
In *Proceedings of the 7th International Conference on Informatics in Control, Automation and Robotics*, pages 5-12
DOI: 10.5220/0002878400050012

airfoils were derived from a laminar WTEA-TE1 reference airfoil (Khalid, 1993, and Khalid, 1993), and were used as a starting point for the actuation system design. The transition point position estimation is made using the information received from a pressure system sensors (optical and Kulite types) equipping the upper face of the wing. Two architectures were developed for morphing system: open loop and closed loop. The difference between the two architectures is given by using or not using the position of transition point as a feedback signal for the actuation lines control. Here described work was developed in the open loop phase; in this phase were made numerical and experimental studies related to the aerodynamics of the morphed wing, to the flexible skin realization, to the actuation system, to the control of the actuation system, and, also, to the real-time determination and visualization of the transition point position using the pressure sensor system. Here, the pressure sensors using is limited to the monitoring of the pressure distribution and of the RMS pressure distribution in the boundary layer.

2 ARCHITECTURE OF THE CONTROLLED MORPHING WING SYSTEM

The chosen wing model was a rectangular one, with a reference airfoil WTEA-TE1, a chord of 0.5 m and a span of 0.9 m. The model was equipped with a flexible skin made of composite materials (layers of carbon and Kevlar fibers in a resin matrix) morphed by two actuation lines (Fig. 1). Each actuation line uses SMA wires as actuators. In the same time, 32 pressure sensors (16 optical sensors and 16 Kulite sensors), were disposed on the flexible skin in different positions along of the chord. The sensors are positioned on two diagonal lines at an angle of 15 degrees from centerline. The rigid lower structure was made from Aluminum, and was designed to allow space for the actuation system and wiring.

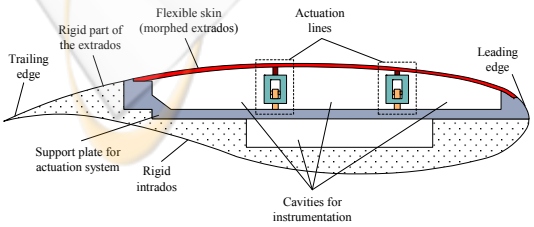

Figure 1: General architecture of the mechanical model.

Starting from the reference airfoil, depending on different flow conditions, 35 optimized airfoils were calculated for the desired morphed positions of the airfoil. The flow conditions were established as combinations of seven incidence angles (-1˚, -0.5˚, 0˚, 0.5˚, 1˚, 1.5˚, 2˚) and five Mach numbers (0.2, 0.225, 0.25, 0.275, 0.3). Each of the calculated optimized airfoils must be able to keep the transition point as much as possible near the trailing edge.

The SMA actuator wires are made of nickel-titanium, and contract like muscles when electrically driven. Also, these have the ability to personalize the association of deflections with the applied forces, providing in this way a variety of shapes and sizes extremely useful to achieve actuation system goals. How the SMA wires provide high forces with the price of small strains, to achieve the right balance between the forces and the deformations, required by the actuation system, a compromise must be established. Therefore, the structural components of the actuation system must be designed to respect the capabilities of actuators to accommodate the required deflections and forces.

Each of our actuation lines uses three shape memory alloys wires (1.8 m in length) as actuators, and contains a cam, which moves in translation relative to the structure (on the x-axis in Fig. 2). The cam causes the movement of a rod related on the roller and on the skin (on the z-axis). The recall used is a gas spring. So, when the SMA is heating the actuator contracts and the cam moves to the right, resulting in the rise of the roller and the displacement of the skin upwards. In contrast, the cooling of the SMA results in a movement of the cam to the left, and thus a movement of the skin down. The horizontal displacement of each actuator is converted into a vertical displacement at a rate 3:1 (results a cam factor c_f=1/3). From the optimized airfoils, an approximately 8 mm maximum vertical displacement was obtained for the rods, so, a 24 mm maximum horizontal displacement must be actuated.

3 SMA ACTUATORS CONTROL DESIGN AND NUMERICAL SIMULATION

The control of SMA actuators can be achieved, in principle, using any method of position control, but the specific properties of SMA actuators, such as hysteresis, the first cycle effect and the long term changes must always be considered. Starting from the established concept of the actuation system the operating schema of the controller can be organized

as is presented in Fig. 3. Based on the 35 studied flight conditions a database of the 35 optimized airfoils can be built. Therefore, for each flight condition results a pair of optimal vertical deflections (dY_{1opt}, dY_{2opt}) for the two actuation lines. The SMA actuators morph the airfoil until the obtained vertical deflections of the two actuation lines (dY_{1real}, dY_{2real}) become equals with the required deflections (dY_{1opt}, dY_{2opt}). The morphed airfoil vertical deflections in the actuation points are measured using two position transducers. The role of the controller is to elaborate an electrical current command signal for the SMA actuators on the base of the error signals (e) between the required vertical displacements and obtained displacements. Because the two actuation lines are identical the designed controller will be valid for both of them.

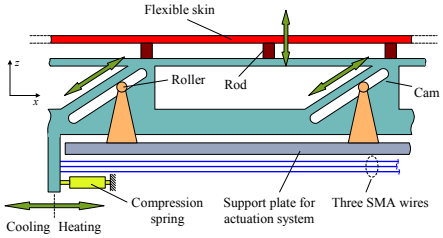

Figure 2: The actuation mechanism concept.

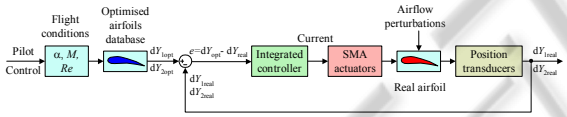

Figure 3: Operating schema of the SMA actuators control.

The first phase of the controller design supposes the numerical simulation of the controlled actuation system. Therefore, a model of SMA actuator was required. In our system a non-linear model was used (a numerical finite element one) build by Prof. P. Terriault using the theoretical model of Lickhatchev (Terriault, 2006). The SMA model has as inputs the initial temperature of the alloy, the electrical current that heats the alloy and the applied force; the outputs are the displacement of the actuator and the temperature of the alloy during functioning. According to this model, to use the shape-changing characteristics the SMA needs to be initialized by an external force, which obliges it to go initially through the transformation phase and further to revert to the initial phase through the cooling phase. Before these two phases, the control can't be realized, due to the intrinsic behavior of the SMA (Terriault, 2006, and Popov, 2008).

Looking the wing as an object moving through the atmosphere, aerodynamic forces are generated between the air and the wing; these forces vary in function of the airflow characteristics (Mach number, Reynolds number and α - angle of attack). Since the aerodynamic forces are suction forces, it tends to lift the skin and to shorten the SMA wire. Against the aerodynamic forces action the elastic force of the flexible skin. A gas spring is needed in order to counteract the aerodynamic forces, so that the resultant force that acts on the SMA wire is given by equation

$$F_{SMA} = F_{spring} + (F_{skin} - F_{aero}) \cdot c_f . \quad (1)$$

To have the premises necessary to initialize the SMA actuators in any conditions, they are loaded by the gas spring even if there are no aerodynamic forces applied on the flexible skin. So, the equation (1) becomes

$$F_{SMA} = (F_{pretension} + k_{spring} \cdot \delta_h) + (k_{skin} \cdot \delta_v - F_{aero}) \cdot c_f , \quad (2)$$

where

$$F_{spring} = F_{pretension} + k_{spring} \cdot \delta_h , \; F_{skin} = k_{skin} \cdot \delta_v . \quad (3)$$

F_{SMA} is the SMA resultant force, F_{spring} - gas spring elastic force, F_{skin} - elastic force produced by the flexible skin, F_{aero} - aerodynamic force, $F_{pretension}$ - pretension force of the spring, c_f - cam factor (1/3), k_{spring} and k_{skin} are the elastic coefficients of the spring, and of the skin, respectively, δ_h and δ_v are the horizontal and vertical actuated displacements.

Implementing the SMA actuators model in a Matlab S-function, the simulation model in Fig. 4 was obtained. As can be observed, to control the SMA actuators, an adequate electrical current must supply it. The length of the SMA wires is a complex function of the SMA load force and temperature, the last one being influenced by the supplying current in time and by the interaction of the wires with the environment in theirs cooling phase (when the electrical supply is removed) (Grigorie, 2009).

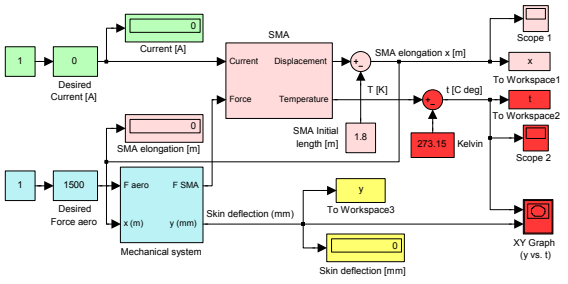

Figure 4: SMA actuators Simulink model.

The block "Mechanical system" in Fig. 4 was modeled accordingly with the equations (1) to (3). As is shown in Fig. 2, the horizontal and the vertical actuated distances are correlated by using the "cam factor" c_f=1/3. Therefore, the aerodynamic and the skin forces (F_{aero} and F_{skin}) are reflected in the SMA load force (F_{SMA}) with the same rate. The gas spring has a preloaded force of 1500 N and a linear elastic coefficient of 2.95 N/mm. In simulations a linear elastic coefficient of approximate 100 N/mm was considered for the skin.

The envelope of the SMA actuator, obtained through numerical simulation for different aerodynamic load cases, is shown in Fig. 5. As can be observed from Fig. 5, to obtain a skin maximum vertical displacement (8 mm) in absence of aerodynamic force, it is required a high temperature (approximately 162˚C) in order to counteract the spring force. Because the ability of the SMA wires to contract is dependent upon Joule heating to produce the transformation temperature required, the need in higher temperature is reflected by a need in higher electrical current. Due to the fact that the aerodynamic forces reduce the actuators load the required current and temperature values are decreased; i.e. for F_{aero}=1800 N the need in temperature for the maximum vertical displacement obtaining is approximately 90˚C. From other point of view, the ability of the SMA wires to return to their original configuration is dependant upon the ability of the system to cool the wires. The simulated SMA model offers just summary information about this subject, the proper heating and cooling of the wires being observed only in the moment of a thermodynamic analysis of the physical morphing wing. The system architecture play a big role in the wire cooling by the convection process, and also the performances of the system can be negatively influenced by heat transfer from actuators to the other components.

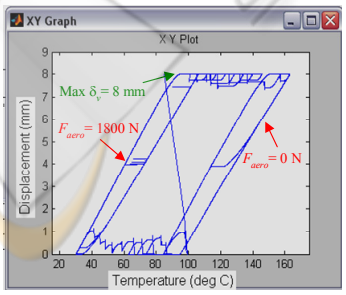

Figure 5: Simulated envelope of the SMA actuator.

According with Fig. 3, the integrated controller purpose is to control the SMA actuators in terms of supply electrical current so that to cancel the deviation e between the required values for vertical displacements (corresponding to the optimized airfoils) and the real values, obtained from position transducers. As mentioned previously, the design of such controller is difficult considering the strong nonlinearities of the SMA actuators characteristics, nonlinearities significantly influenced by the forces with which they are tense. The chosen design procedure consisted of the following steps:

Step 1: numerical simulation of the SMA model actuators for certain values of the forces in the system;

Step 2: approximation of the system with linear systems in the heating and cooling phases using the System Identification Toolbox of Matlab and the numerical values obtained at the Step 1;

Step 3: the choice of the controller type and its tuning for each of the two SMA actuators phase – heating and cooling;

Step 4: the integration of the two obtained controller in a single one followed by its validation for the general model of the system (non-linear).

Because the team that established the actuation line architecture (Georges, 2009) suggested that the pretension force of the gas spring must have the value $F_{pretension}$=1500 N, F_{aero}= 1500 N value was chosen in numerical simulations for the aerodynamic force. Simulating a cooling phase followed by a heating phase with the model in Fig. 4, the blue characteristics depicted in Fig. 6 were obtained. In the first graphical window of the figure is presented the SMA wire length changing in time (δ_h), while in the second window the SMA wire temperature values in the two phases are shown. One observes that a SMA wire dilatation results in the cooling phase, and a wire contraction is obtained in the heating phase. For a horizontal actuation distance of approximately 24 mm the wire temperature reaches a value near by 100˚C. Note are the transient time to reach the steady-state values for the two phases: approximate 60 s for the cooling phase and approximate 40 s for the heating phase. For the steady-state, after the cooling phase, the numerical simulation obtained forces were: F_{SMA}=1000 N, F_{skin}=0 N and F_{spring}=1500 N. In this steady-state the system is relaxed in terms of mechanical and the vertical displacement of the actuator is null. For the steady-state, after the cooling phase, the numerical simulation obtained forces were: F_{SMA}=1337 N, F_{skin}=266.1 N and F_{spring}=1571 N. This steady-state corresponds to the actuation system maximal vertical displacement of approximately 8 mm.

Using the Matlab System Identification Toolbox

and the numerical values characterizing the δ_h response at a series of successive step inputs, two transfer functions were found for the SMA phases:

$$H_h(s) = \frac{0.0177388 \cdot s^2 + 0.004017 \cdot s + 0.0241958}{s^3 - 1.43582 \cdot s^2 + 0.64742 \cdot s - 0.001018},$$
$$H_c(s) = \frac{0.3535 \cdot s + 0.2672}{s^2 - 1.9386 \cdot s + 0.011242}, \quad (4)$$

where $H_h(s)$ and $H_c(s)$ are the transfer functions for heating and cooling phases. The displacements δ_h, corresponding to the linear systems obtained through the two phases identification, are depicted with red line in Fig. 6. A very good approximation can be also observed for the two phases through the identification in simulated conditions. The previously established transfer functions help to the controller type choice for each phase and to its tuning.

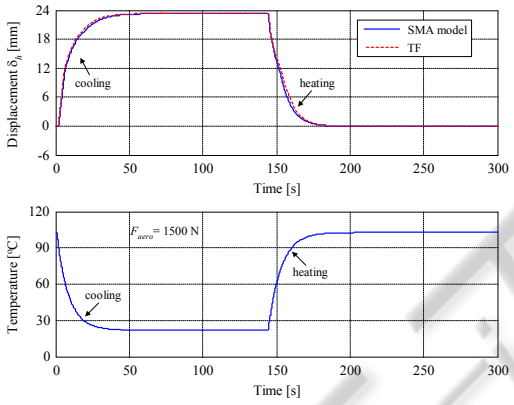

Figure 6: Actuator displacement and temperature vs time.

Considering the significance of physical controlled phenomenon, that the SMA wire must be heated to contract and then cooled to dilate by providing an appropriate electrical current by the control block, it is normal that in the cooling phase the actuators not be powered. This phase of cooling may occur in controlling not only a long-term phase, when it ordered a switch between two values of the actuator displacements, but also as a short-lived phase, which occurs when the real value of the deformation exceeds its desired value and is need to cool the actuator wires. On the other hand, it is imperative that in the heating phase actuators to be controlled so that the stationary error of the automatic system to be zero. Therefore, for this phase one opted for a simple architecture of the controller of PI type (proportional-integral). It combines the advantages of proportional type controller, which reduces substantially the overshoot and lead to a short transient time, with the benefits of the integral controller, which cancels the steady-state system error. As a consequence, the resulted controller must behave like a switch between cooling phase and heating phase, situations where the output current is 0 A, or is controlled by a law of PI type. The two phase's interconnection leads to an integrated controller, which can be viewed as a combination of a bi-positional controller (an on-off one) and a PI (proportional-integral) controller.

The input-output characteristic of a bi-positional (on-off) controller can be described by the equation

$$i(t) = \begin{cases} -i_m, \text{ if } e \le 0, \\ i_m, \text{ if } e > 0, \end{cases} \quad (5)$$

where $i(t)$ is the command variable (electrical current in our case) in time, i_m reflects the value of the command and e is the operating error (Fig. 3). The PI controller law is given by

$$i(t) = K_P \cdot e(t) + K_I \cdot \int e(t) \cdot dt, \quad (6)$$

with K_P - the proportional gain, and K_I - the integral gain. Combining the two controllers in a single one, based on the rules previously mentioned results the control law of the integrated controller as the form

$$i(t) = \begin{cases} 0, \text{ if } e \le 0, \\ K_P \cdot e(t) + K_I \cdot \int e(t) \cdot dt, \text{ if } e > 0. \end{cases} \quad (7)$$

The optimal tuning of the controller in heating phase was realized using an integral criterion, the error minimum surface criterion, very well known in the literature as Ziegler-Nichols criterion (Mihoc, 1980); the tuning methodology is: a) the regulator is considered as a proportional one (P) and it is tuned with respect to the K_P parameter; b) the amplification factor K_P is increased until the response of the automatic system will be self-sustained oscillatory. One memorizes the value K_{P0} of K_P for which the system has an oscillatory behavior and the value of oscillations semi-period (T_0). The optimal values for the parameters of the PI regulator are determined using the relations:

$$K_P = 0.45 \cdot K_{P0}, \quad K_I = K_P / (0.85 \cdot T_0). \quad (8)$$

Follows the controller tuning steps the next numerical values for the PI controller parameters were obtained and/or were calculated:

$$K_{P0} = 3984, \; T_0 = 2.68\text{s}, \\ K_P = 1792.8, \; K_I = 787.0061. \quad (9)$$

As a consequence, the controlled system in hea-

ting phase can be modeled with an approximate linear system with the block schema in Fig. 7. The parameters $a_0 \div a_2$ and $b_0 \div b_3$ in the schema are the coefficients of the $H_h(s)$ transfer function nominator and denominator in ascending power of s (eq. (4)). The open loop transfer function of the controlled heating phase is

$$H_{ol}(s) = C_{PI}(s) \cdot H_h(s) = \frac{q_3 s^3 + q_2 s^2 + q_1 s + q_0}{b_3 s^4 + b_2 s^3 + b_1 s^2 + b_0 s}, \quad (10)$$

while the closed loop transfer function is

$$H_{cl}(s) = C_{PI}(s) \cdot H_h(s) = \frac{q_3 s^3 + q_2 s^2 + q_1 s + q_0}{r_4 s^4 + r_3 s^3 + r_2 s^2 + r_1 s + r_0}. \quad (11)$$

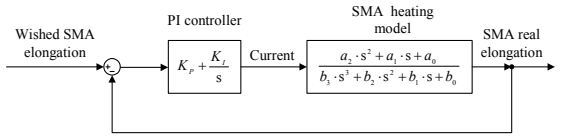

Figure 7: The block schema with transfer functions of the heating phase linear model.

The included coefficients are

$$\begin{aligned} &q_3 = K_P a_2 = 31.8021, \quad q_2 = K_P a_1 + K_I a_2 = 21.1622, \\ &q_1 = K_P a_0 + K_I a_1 = 46.5396, \; q_0 = K_I a_0 = 19.0422, \end{aligned} \quad (12)$$

respectively

$$\begin{aligned} &r_4 = b_3 = 1, \; r_3 = b_2 + K_P a_2 = 30.3663, \\ &r_2 = b_1 + K_P a_1 + K_I a_2 = 21.8096, \\ &r_1 = b_0 + K_P a_0 + K_I a_1 = 46.5386, \; r_0 = K_I a_0 = 19.0422. \end{aligned} \quad (13)$$

$C_{PI}(s)$ is the transfer function of the PI controller. The poles of the close loop transfer function $H_{cl}(s)$ result with the values

$$\begin{aligned} &p_1 = -29.6837, \; p_1 \in \mathbf{R}_-, \; p_4 = -0.4453, \; p_1 \in \mathbf{R}_- \\ &p_2 = -0.1187 + 1.1943 \cdot i, \; p_2 \in \mathbf{C}, \; \mathrm{Re}(p_2) \in \mathbf{R}_-, \\ &p_3 = -0.1187 - 1.1943 \cdot i, \; p_3 \in \mathbf{C}, \; \mathrm{Re}(p_3) \in \mathbf{R}_-. \end{aligned} \quad (14)$$

One can observe that all poles of the transfer function are placed in the left-hand side of the s-plane, and the obtained system is stable.
In the state-space representation

$$\begin{aligned} \dot{\mathbf{x}}(t) &= A\mathbf{x}(t) + B\mathbf{u}(t), \\ \mathbf{y}(t) &= C\mathbf{x}(t) + D\mathbf{u}(t), \end{aligned} \quad (15)$$

the state matrix A, the input matrix B, the output matrix C and the feed-forward matrix D, were obtained by the forms

$$A = \begin{bmatrix} -30.3663 & -21.8096 & -46.5386 & -19.0422 \\ 1 & 0 & 0 & 0 \\ 0 & 1 & 0 & 0 \\ 0 & 0 & 1 & 0 \end{bmatrix}, \quad (16)$$

$$B^T = [1 \; 0 \; 0], \; C = [31.8 \; 21.1 \; 46.5 \; 19], \; D = 0.$$

Evaluating the controllability and observability of the system (P and Q matrices) results

$$P = \begin{bmatrix} 1 & -30.3663 & 900.3025 & -26723.119 \\ 0 & 1 & -30.3663 & 900.3025 \\ 0 & 0 & 1 & -30.3663 \\ 0 & 0 & 0 & 1 \end{bmatrix}, \quad (17)$$

$$Q = \begin{bmatrix} 31.8 & 21.1 & 46.5 & 19 \\ -944.5 & -647 & -1460.9 & -605.5 \\ 28035.4 & 19139.3 & 43352.4 & 17986.3 \\ -832193.6 & -568090.6 & -1286744.7 & -533857.8 \end{bmatrix}; \quad (18)$$

$$\mathrm{rank}(P) = \mathrm{rank}(Q) = \text{system order} = 4. \quad (19)$$

As a consequence, the system is completely controllable and observable.

Based on the previously considerations, the final form of the integrated controller law is

$$i(t) = \begin{cases} 0, \text{ if } e \le 0, \\ 1792.8 \cdot e(t) + 787.0061 \cdot \int e(t) \cdot \mathrm{d}t, \text{ if } e > 0. \end{cases} \quad (20)$$

Introducing the controller in a general block schema, with the non-linear SMA model, the Simulink model in Fig. 8 was obtained for the SMA actuators control (see Fig. 3). The input variable of the schema is the desired skin deflection and the output is the real skin deflection.

The "Integrated controller" block contains the implementation of the law described by equation (20) and of the preliminary observations related to the SMA actuators physical limitations in terms of temperature and supplying currents. Its schema is shown in Fig. 9. The inputs of the block are the control error (difference between the desired and the obtained displacements) and the wires temperature, and the output is controlled electrical current applied on the SMA actuators. There are two switches in the schema; the first one chooses one of the two options in the control law (20) and the second one switching the electrical current value to 0A when the SMA temperature value is over the imposed limit. Also, a current saturation block is used to prevent the current increase over the physical limit supported by the actuation SMA wires.

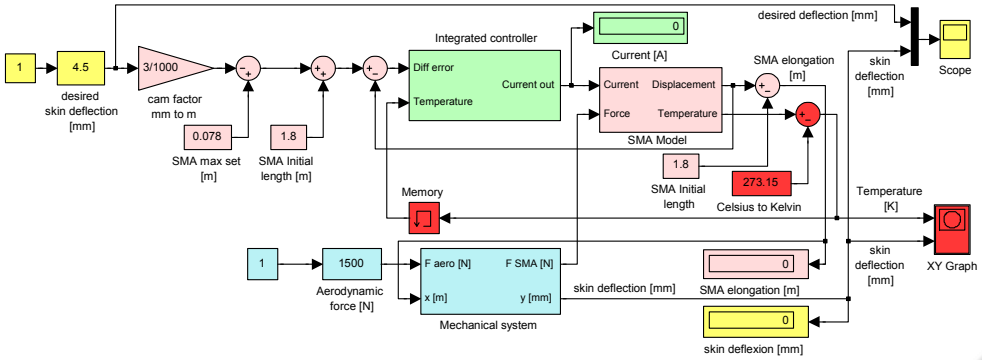

Figure 8: The simulation model for the controlled SMA actuator with non-linear model.

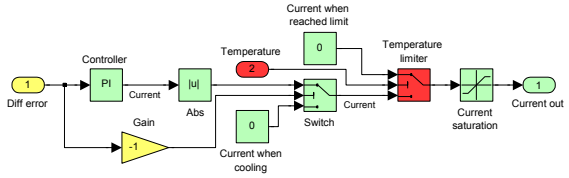

Figure 9: "Integrated controller" block in Simulink.

Loading the simulated model with aerodynamic force F_{aero} = 1500N, the characteristics in Fig. 10 are obtained for a 6 mm step desired skin deflection (δ_v). First of all, can be observed that the controller work good, the transition to the desired steady-state being significantly improved through the integration of the two control law in the equation (20): 1) the amplitudes of oscillations were reduced and the observed oscillations in the SMA temperatures around the steady-state are due only to the thermal inertia of the smart material; 2) the values of the transition time from 0mm to the steady-state values decrease from 20÷25 to approximate 5 s.

4 CONCLUSIONS

The objective of here presented research work is to develop an actuation control concept for a new morphing mechanism using smart materials, like Shape Memory Alloy (SMA), as actuators. These smart actuators modify the upper surface of a wing made of a flexible skin so the laminar to turbulent transition point moves close to the wing airfoil trailing edge.

The designed controller must controls the SMA actuators in terms of supply electrical current so that to cancel the deviation between the required values for vertical displacements (corresponding to the optimized airfoils) and the real values, obtained from position transducers. The envelope of the SMA actuator in Fig. 5, obtained through numerical simulation using model in Fig. 4 for different aerodynamic load cases, confirms that the length of the SMA wires is a complex function of the SMA load force and temperature, the last one being influenced by the supplying current in time and by the interaction of the wires with the environment in theirs cooling phase (when the electrical supply is removed).

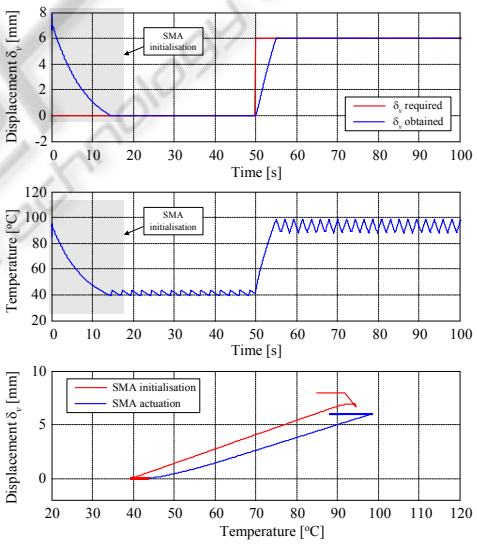

Figure 10: Response for a step input and F_{aero}=1500 N.

As can be observed from Fig. 5, to obtain a skin maximum vertical displacement (8 mm) in absence of aerodynamic force, it is required a high temperature (approximately 162˚C) in order to counteract the spring force. Because the ability of the SMA wires to contract is dependent upon Joule heating to produce the transformation temperature required, the need in higher temperature is reflected by a need in higher electrical current. Due to the fact that the aerodynamic forces reduce the actuators load the required current and temperature values are

decreased; i.e. for F_{aero}= 1800 N the need in temperature for the maximum vertical displacement obtaining is approximately 90˚C.

The final configuration of the integrated controller was a combination of a bi-positional controller (particularly an on-off one) and a PI (proportional-integral) controller, due to the two phases (heating and cooling) of the SMA wires interconnection. The resulted controller must behave like a switch between cooling phase and heating phase, situations where the output current is 0 A, or is controlled by a law of PI type.

Using an integral criterion, the error minimum surface criterion (Ziegler-Nichols), the PI controller for the heating phase was optimal tuned, the resulted values are K_P=1792.8 and K_I=787.0061. Evaluating the systems' performances one observed that the poles of closed loop transfer function of the controlled heating phase resulted with the values (14) are all placed in the left-hand side of the s-plane, so the obtained system is stable. On the other way, the system was found to be completely controllable and observable based on the values established in equations (17)÷(19). So, the final form of the integrated controller law was (20).

Loading the numerically simulated general model (the non-linear one with $F_{pretension}$=1500N) in Fig. 8 with aerodynamic force F_{aero} = 1500N, the obtained characteristics in Fig. 10 confirm that the controller works good, the transition to the desired steady-state being significantly improved through the integration of the two control law in the equation (20): 1) the amplitudes of oscillations were reduced and the observed oscillations in the SMA temperatures around the steady-state are due only to the thermal inertia of the smart material; 2) the values of the transition time from 0mm to the steady-state values decrease from 20÷25 to approximate 5 s.

As second and third validation methods a bench test and a wind tunnel test were performed and will be presented in the second part of the paper, related to the experimental validation.

ACKNOWLEDGEMENTS

We would like to thank the Consortium of Research in the Aerospatial Industry in Quebec (CRIAQ), Thales Avionics, Bombardier Aerospace, and the National Sciences and Engineering Research Council (NSERC) for the support that made this research possible. We would also like to thank George Henri Simon for initiating the CRIAQ 7.1 project and Philippe Molaret from Thales Avionics and Eric Laurendeau from Bombardier Aeronautics for their collaboration on this work.

REFERENCES

Chang, P., Shah, A., Singhee, M., 2009, *Parameterization of the Geometry of a Blended Wing Body Morphing Wing*, Project report, Georgia Institute of Technology, April 2009, Atlanta, Georgia, USA

Georges, T., Brailovski, V., Morellon, E., Coutu, D., Terriault, P., 2009, *Design of Shape Memory Alloy Actuators for Morphing Laminar Wing With Flexible Extrados*, Journal of Mechanical Design, Vol. 31, Nº 9

Gonzalez, L., 2005, *Morphing Wing Using Shape Memory Alloy: a concept proposal*, Final research paper, Texas A&M University, College Station, Texas, USA

Grigorie, T. L., Botez, R. M., 2009, *Adaptive neuro-fuzzy inference system-based controllers for smart material actuator modeling*, Journal of Aerospace Engineering, Vol. 223, No. 6, pp. 655-668

Hinshaw, T. L., 2009, *Analysis and Design of a Morphing Wing Tip using Multicellular Flexible Matrix Composite Adaptive Skins*, Master of Science Thesis, Virginia Polytechnic Institute and State University, Virginia, USA

Khalid, M., Jones, D. J., 1993, *Navier Stokes Investigation of Blunt Trailing Edge Airfoils using O-Grids*, AIAA Journal of Aircraft, vol.30, no.5, pp. 797-800

Khalid, M., Jones, D. J., 1993, *A CFD Investigation of the Blunt Trailing Edge Airfoils in Transonic Flow*, Inaugural Conference of the CFD Society of Canada.

Majji, M., Rediniotis, O. K., Junkins, J.L., 2007, *Design of a Morphing Wing: Modeling and Experiments*, AIAA Atmospheric Flight Mechanics Conference and Exhibit, Hilton Head, South Carolina, USA

Mihoc, D., 1980, *Teoria si elementele sitemelor de reglare automata*. Editura Didactica si Pedagogica, Bucuresti

Namgoong, H., Crossley, W. A., Lyrintzis, A. S., 2006, *Aerodynamic Optimization of a Morphing Airfoil Using Energy as an Objective*, 44th AIAA Aerospace Sciences Meeting and Exhibit, Reno, Nevada, USA

Popov, A. V., Labib, M., Fays, J., Botez, R. M., 2008, *Closed-Loop Control Simulations on a Morphing Wing*, Journal of Aircraft, Vol. 45, pp. 1794-1803

Ruotsalainen, P., et. al., 2009, *Shape Control of a FRP Airfoil Structure Using SMA-Actuators and Optical Fiber Sensors.* Journal of Solid State Phenomena, Volume 144, pp. 196-201

Smith, K., Butt, J., Spakovsky, M. R., Moorhouse, D., 2007, *A Study of the Benefits of Using Morphing Wing Technology in Fighter Aircraft Systems*, 39th AIAA Thermophysics Conference, Miami, Forida, USA

Terriault, P., Viens, F., Brailovski, V., 2006, *Non-isothermal Finite Element Modeling of a Shape Memory Alloy Actuator Using ANSYS*, Computational Materials Science, Vol. 36, No. 4, pp. 397-410